NRC Research Press

ARTICLE

Correcting the nondetection bias of angle count sampling

Tim Ritter, Arne Nothdurft, and Joachim Saborowski

Abstract: The well-known angle count sampling (ACS) has proved to be an efficient sampling technique and has been applied in forest inventories for many decades. However, ACS assumes total visibility of objects; any violation of this assumption leads to a nondetection bias. We present a novel approach, in which the theory of distance sampling is adapted to traditional ACS to correct for the nondetection bias. Two new estimators were developed based on expanding design-based inclusion probabilities by model-based estimates of the detection probabilities. The new estimators were evaluated in a simulation study as well as in a real forest inventory. It is shown that the nondetection bias of the traditional estimator is up to –52.5%, whereas the new estimators are approximately unbiased.

Résumé : L'échantillonnage par balayage sous angle constant (EAC) est une technique d'échantillonnage bien connue qui s'est avérée efficace et qui a été appliquée dans les inventaires forestiers pendant de nombreuses décennies. Toutefois, l'EAC assume que tous les objets sont visibles et toute violation de cette hypothèse entraîne un biais de non-détection. Nous présentons une nouvelle approche qui consiste à adapter la théorie de l'échantillonnage selon la distance à l'EAC traditionnel pour corriger le biais de non-détection. Deux nouveaux estimateurs ont été créés en complétant les probabilités d'inclusion basées sur le plan de sondage par les probabilités de détection basées sur un modèle. Les nouveaux estimateurs ont été évalués par une étude de simulation ainsi que par un inventaire forestier réel. Les résultats montrent que le biais de non-détection de l'estimateur traditionnel peut atteindre –52,5 %, alors que les nouveaux estimateurs sont presque exempts de biais. [Traduit par la Rédaction]

Introduction

The well-known angle count sampling (ACS) (Bitterlich 1984, 1952) has proved to be an efficient sampling technique for forest inventories. It is used in several national forest inventories, for example, in Germany (Polley 2005; Kändler 2009), Finland (Tomppo 2009), and Austria (Gabler and Schadauer 2006; Schadauer et al. 2007).

However, ACS assumes total visibility of objects; any violation of this assumption leads to a nondetection bias. Especially when sampling rare objects such as admixed tree species or deadwood, this bias is relatively more important.

Since rare objects are often of high ecological value, their frequency is considered as an important indicator for assessing environmental sustainability of forest management. Therefore, the development of efficient sampling techniques for surveying rare objects gains more and more importance nowadays. For example, deadwood assessments are increasingly included in national-scale forest inventories (Woodall et al. 2009*a*). As the "Volume of standing deadwood and of lying deadwood on forest and other wooded land classified by forest type" is one of the "Pan-European criteria and indicators for sustainable forest management" defined by the 4th Ministerial Conference on the Protection of Forests in Europe (MCPFE 2002, 2003), 21 European countries have included deadwood sampling in their national forest inventories (Rondeux and Sanchez 2010). In 30 countries around the globe, and on more than a third of the world's forestland, deadwood is surveyed. Almost all of these countries use fixed area sampling (FAS) for surveying standing deadwood. For sampling downed deadwood, FAS and line intersect sampling (LIS) are the most popular methods (Woodall et al. 2009*a*, 2009*b*). However, as the occurrence of deadwood in managed forests can be regarded as a stochastically rare event with strong clumping and high local variability (Meyer 1999), FAS is a very inefficient sampling technique for deadwood (Ritter and Saborowski 2012), as well as for other objects having similar characteristics.

ACS may be a more efficient alternative, but suffers from the nondetection bias. Gove et al. (2001), for example, reported about severe problems with the nondetection bias when sampling coarse woody debris with an adapted version of ACS. They considered a three-person sampling team to be optimal, because two of three persons can traverse the plot in search of coarse woody debris to overcome the problem of nondetection bias. However, for large inventories this approach seems to be a rather inefficient and cost intensive.

In this paper we present a new approach for correcting the nondetection bias often occurring when sampling rare objects with traditional ACS under limited sight conditions. For the proposed estimators, the well-established theory on distance sampling (Buckland et al. 2001, 2004) is combined with the estimator for traditional ACS to account for the nondetection bias. Performance of the estimators is examined in a field study in comparison with FAS as reference and in an exhaustive simulation study, where the new estimators are applied to simulated tree patterns.

Sampling methods and estimators

Angle count sampling (ACS)

At each sample plot in an arbitrary forest, each tree has to be targeted with the relascope. A tree is counted if its diameter at 1.3 m in height (DBH) appears to be wider then the marks of the relascope.

According to Bitterlich (1984), the mean basal area of trees per area unit in a forest (G) can be estimated from the number of trees (z_i) counted at a randomly selected point i and the basal area factor (k).

Received 2 October 2012. Accepted 19 January 2013.

T. Ritter. University of Göttingen, Department of Ecoinformatics, Biometrics and Forest Growth, Büsgenweg 4, Göttingen 37077, Germany.
A. Nothdurft. Forest Research Institute Baden-Württemberg, Department of Biometrics and Informatics, Post Box 79007, Freiburg 79100, Germany.
J. Saborowski. University of Göttingen, Department of Ecoinformatics, Biometrics and Forest Growth, Büsgenweg 4, Göttingen 37077, Germany; University of Göttingen, Department of Ecosystem Modelling, Büsgenweg 4, Göttingen 37077, Germany.
Corresponding author: Tim Ritter (email: tritter@gwdg.de).

[1] $G_i = z_i k$

The basal area factor in $m^2 \cdot ha^{-1}$ per counted tree

[2] $k = 10\,000 \sin^2\left(\frac{\alpha}{2}\right) = \frac{d^2}{4R^2} = \frac{\frac{\pi}{4}d^2}{\pi R^2}$

is given by the basal area density of a single tree in its marginal circle, where d is the DBH of the tree (measured in cm), R is the radius of the marginal circle (measured in m) and α is the corresponding critical angle of the relascope. For a survey with n sample plots, G can be estimated as the sample mean of all G_i.

[3] $\hat{G}_{ACS} = \frac{1}{n}\sum_{i=1}^{n} G_i = \frac{k}{n}\sum_{i=1}^{n} z_i$

$\hat{G}_{ACS}$ is unbiased as long as the trees are completely recorded. However, owing to limited sighting conditions some trees are not detected and $\hat{G}_{ACS}$ is therefore biased in practice.

Point transect sampling (PTS)

The necessary sampling effort for PTS (Buckland et al. 2001) is very small, because only the distances r_{ij} from the center of every sample plot i to any object j sighted from that point have to be measured (e.g., by laser rangefinder) and recorded. Please note that, to keep in line with the notation of Bitterlich (1984), we use a slightly different notation than Buckland et al. (2001); in particular, n is used instead of k for the number of sample plots and m is used instead of n for the number of objects encountered. PTS is usually applied for the estimation of the object density D (i.e., the number of trees per area unit) based on the number of sighted objects m, the number of point transects n, and the probability

[4] $P_a = \frac{2}{\omega^2}\int_0^{\omega} rg(r)\mathrm{d}r$

that a randomly chosen object is detected within a circle of radius ω and area $a = \pi\omega^2$. The crucial point at the concept of PTS is to estimate the so-called detection function $g(r)$, which gives the probability that an object is detected given that its location has a distance r from the sample point. The basic assumption is that an object located directly at the sample point ($r = 0$) is detected with certainty ($g(0) = 1$), and that the detection probability decreases with increasing r. The parameters of $g(r)$ can be estimated by fitting a model to the distribution of observed r using a maximum likelihood approach. $g(r)$ can be normalized to the probability density function $f(r) = rg(r)/\int_0^{\omega} rg(r)\mathrm{d}r$. The PTS estimator according to Buckland et al. (2001) is

[5] $\hat{D} = \frac{m}{n\pi\omega^2\hat{P}_a}$

or equivalently

[6] $\hat{D} = \frac{m\hat{h}(0)}{2\pi n}$

where $\hat{h}(0) = 1/\int_0^{\omega} r\hat{g}(r)\mathrm{d}r$ is actually the slope of the probability density function $\hat{f}(r)$ evaluated at $r = 0$ (Buckland et al. 2001).

The best model for estimating $g(r)$ is selected based on the minimum Akaike information criterion (AIC) (Buckland et al. 2001).

As shown in Buckland et al. (2001) and under the assumption that the two variance components are uncorrelated, the variance estimator

[7] $\widehat{\mathrm{var}}(\hat{D}) = \hat{D}^2\left\{\frac{\widehat{\mathrm{var}}(m)}{m^2} + \frac{\widehat{\mathrm{var}}[\hat{h}(0)]}{[\hat{h}(0)]^2}\right\}$

can be derived using the delta method (Seber 1982).

For the estimation of var(m), we applied a model-based variance estimator (Fewster et al. 2009) that simply becomes

[8] $\widehat{\mathrm{var}}(m) = \frac{1}{n-1}\sum_{i=1}^{n}(m_i - \bar{m})^2$

because of the fact that, during a sampling campaign, every sample plot was visited exactly once. Please note that also in contrast with Fewster et al. (2009) we use n instead of k for the number of point transects and m instead of n for the number of observed objects.

Using a half-normal detection function having a single parameter σ^2, the maximum likelihood estimator of var $[\hat{h}(0)]$ becomes

[9] $\widehat{\mathrm{var}}[\hat{h}(0)] = \frac{1}{m\hat{\sigma}^4} = \frac{[\hat{h}(0)]^2}{m}$

(Buckland et al. 2001). For more details please refer to chapter 3.3 in Buckland et al. (2001).

Bias-corrected angle count sampling (BcACS) – Heuristic approach

Estimator 1 (BcACS1)

If the distance r_{ij} from the center of plot i to every sighted tree j that is supposed to be counted by ACS is measured, one may use the first bias-corrected ACS estimator. Assuming $g(r)$ as a model for the distance-dependent detection probability and substituting z_i by $\sum_{j=1}^{z_i}\frac{1}{\hat{g}(r_{ij})}$ in the ACS formula (eq. [3]), gives a bias-corrected estimation of the basal area of trees per area unit G.

[10] $\hat{G}_{BcACS1} = \frac{k}{n}\sum_{i=1}^{n}\sum_{j=1}^{z_i}\frac{1}{\hat{g}(r_{ij})}$

Thus, each tree count is individually expanded by the tree's inverse estimated detection probability to correct for the negative bias introduced by overlooking trees.

Estimator 2 (BcACS2)

If the diameter of each counted tree is additionally measured, one may use an alternative bias-corrected estimator that involves the overall distance-independent probability ($P_{a_{ij}}$) for the marginal circle of each tree. Diameter and height of every counted tree were measured for example in the repeated German national forest inventories to estimate volume increment (Polley 2005). In that case, measuring all r_{ij} is not necessary as long as enough measurements are taken to estimate $g(r)$ or an estimate $\hat{g}(r)$ is known from an earlier inventory.

From the ACS theory it is known that the radius of the marginal circle in which a tree with DBH d_{ij} is counted is given by $R_{ij} = d_{ij}/(2\sqrt{k})$ (see eq. [2]). Substituting ω by R_{ij} in eq. [4] yields

[11] $P_{a_{ij}} = \frac{2}{R_{ij}^2}\int_0^{R_{ij}} rg(r)\mathrm{d}r$

Fig. 1. Number of sampled objects per plot for the different sampling techniques.

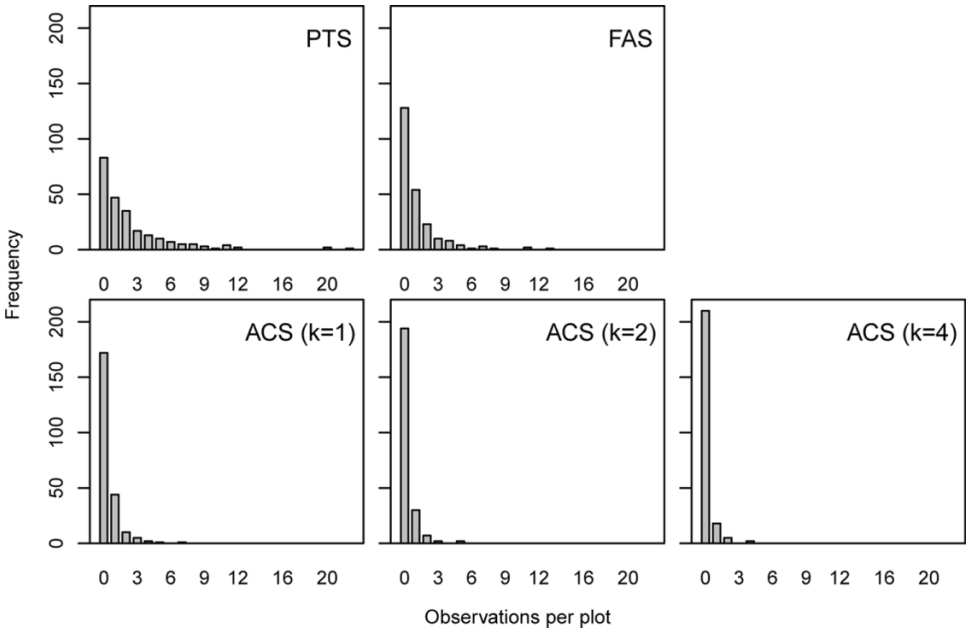

Fig. 2. Empirical diameter distributions of standing deadwood sampled with the different sampling techniques. Please note the different scaling of the *y* axes.

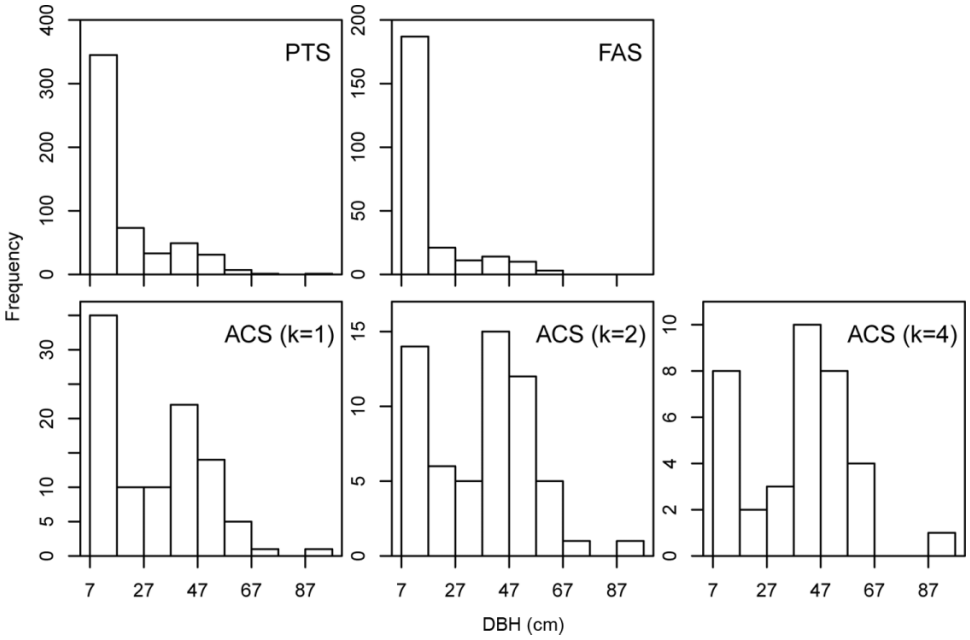

the probability to detect a tree with DBH d_{ij} from a random point within its marginal circle. In other words, $P_{a_{ij}}$ is the mean detection probability of all trees that have DBH d_{ij} and that are supposed to be counted. "Supposed to be counted" means that the distance of that tree from the sample plot center is smaller than or equal to the radius of its individual marginal circle R_{ij}.

Similar to the derivation of eq. [10], we substitute z_i by $\sum_{j=1}^{z_i} \frac{1}{\hat{P}_{a_{ij}}}$ in the ACS formula (eq. [3]), which is equivalent with replacing $\hat{g}(r_{ij})$ by $\hat{P}_{a_{ij}}$ in eq. [10]. These arguments lead to the second bias-corrected estimator.

$$\hat{G}_{\mathrm{BcACS2}} = \frac{k}{n}\sum_{i=1}^{n}\sum_{j=1}^{z_i}\frac{1}{\hat{P}_{a_{ij}}} = \frac{1}{n}\sum_{i=1}^{n}\sum_{j=1}^{z_i}\frac{d_{ij}^2}{4R_{ij}^2\hat{P}_{a_{ij}}} \quad [12]$$

The second equality follows from $k = d_{ij}^2/(4R_{ij}^2)$ (see eq. [2]). Thus, each counted tree contributes with its basal area per area unit expanded by the inverse estimated mean detection probability of all trees that have the same DBH d_{ij} and are supposed to be counted at any sample point.

Fig. 3. Estimated half-normal detection function ($\hat{g}(r)$) and normalized density of observed objects in different distances. The original density is normalized by dividing the density of detected objects in every distance interval by the estimated density of all objects ($\hat{D}$) as shown in Buckland et al. (2001). Please note that normalized densities are not detection probabilities and, therefore, can be greater than 1.

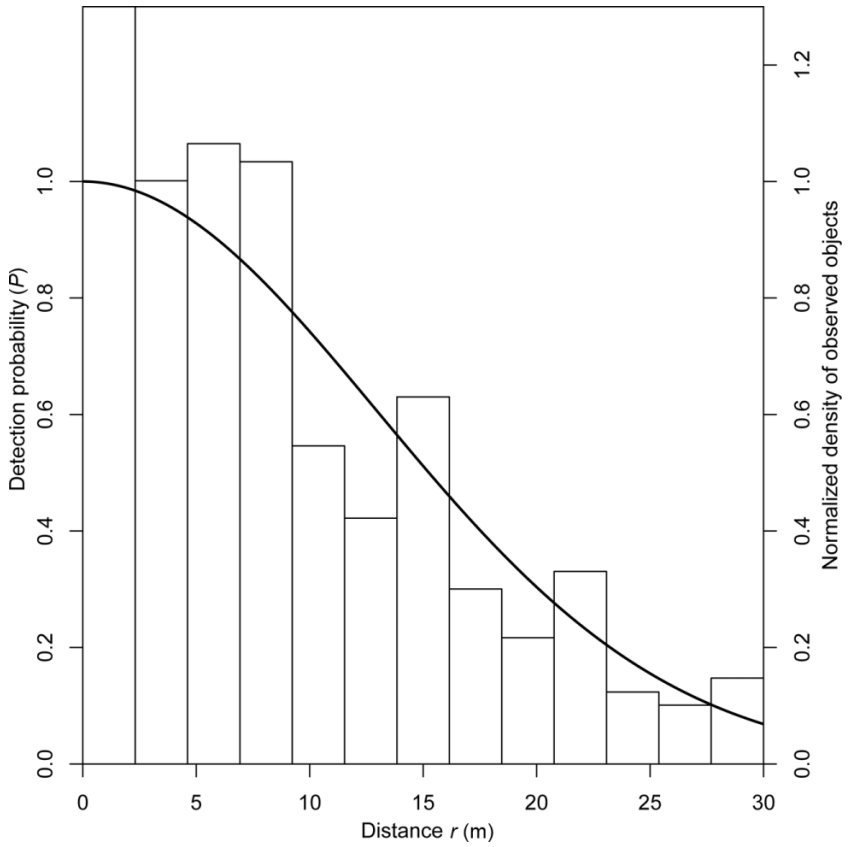

Theoretical justification of suggested bias corrections

For simplicity, we focus on one sample point i at location x, which allows the removal of subscript i in the formulas. Furthermore, we assume that ACS is carried out according to the so-called buffer method (Gregoire and Valentine 2008) to account for the well-known boundary problems. Thus, the population total of response variable Y over N trees

$$[13] \qquad Y = \sum_{j=1}^{N} Y_j$$

can be estimated using the unbiased Horvitz–Thompson estimator

$$[14] \qquad \hat{Y}(x) = \sum_{j=1}^{z} \frac{Y_j}{\pi_j} \quad \text{with} \quad \pi_j = \frac{\pi R_j^2}{A^*}$$

where A^* is the area of the forest to be inventoried (A) extended by the area of the peripheral zone (Gregoire and Valentine 2008; Mandallaz 2008) and $R_j = d_j/(2\sqrt{k})$. Please note the different symbols π and π for the inclusion probability and for the circle constant, respectively.

If one takes into account that the trees that are supposed to be counted (i.e., x lies in their marginal circle K_j of radius R_j) may be overlooked, the inclusion probability π of tree j is no longer valid and must be corrected. Assuming that the detection probability of tree j, located at distance r_j from sample point x, can be described by a detection function $g(r_j)$, the new inclusion probability is

Table 1. Comparison of estimated basal area of standing deadwood per area unit ($\hat{G}$, m²·ha⁻¹) for the different sampling methods and corresponding $\widehat{\text{SE}}$s (m²·ha⁻¹).

Estimator	k	$\hat{G}$	$\widehat{\text{SE}}(\hat{G})$
ACS	1	0.421	0.059
BcACS1	1	0.609	0.095
BcACS2	1	0.686	0.107
ACS	2	0.511	0.090
BcACS1	2	0.689	0.134
BcACS2	2	0.701	0.128
ACS	4	0.614	0.137
BcACS1	4	0.714	0.162
BcACS2	4	0.732	0.164
FAS	—	0.654	0.117

Note: k, basal area factor; $\widehat{\text{SE}}$, estimated standard error; ACS, angle count sampling; FAS, fixed area sampling; BcACS, bias-corrected angle count sampling stimator.

$$[15] \qquad \begin{aligned} \pi_j^+ &= P(\{x \in K_j\} \cap \{j \text{ is detected}\}) \\ &= P(x \in K_j)P(j \text{ is detected} | x \in K_j) = \pi_j P_{a_j} \end{aligned}$$

This leads to the unbiased estimator

$$[16] \qquad \begin{aligned} \hat{Y}(x) &= \frac{1}{A^*} \sum_{j=1}^{z} \frac{Y_j}{\pi_j^+} = \sum_{j=1}^{z} \frac{Y_j}{\pi R_j^2 P_{a_j}} \\ &= k \sum_{j=1}^{z} \frac{Y_j}{(\pi/4) d_j^2 P_{a_j}} \end{aligned}$$

of the Y total per area unit, which simplifies to

Fig. 4. Exemplary realizations of simulated point processes and boundaries of outer and inner simulation windows.

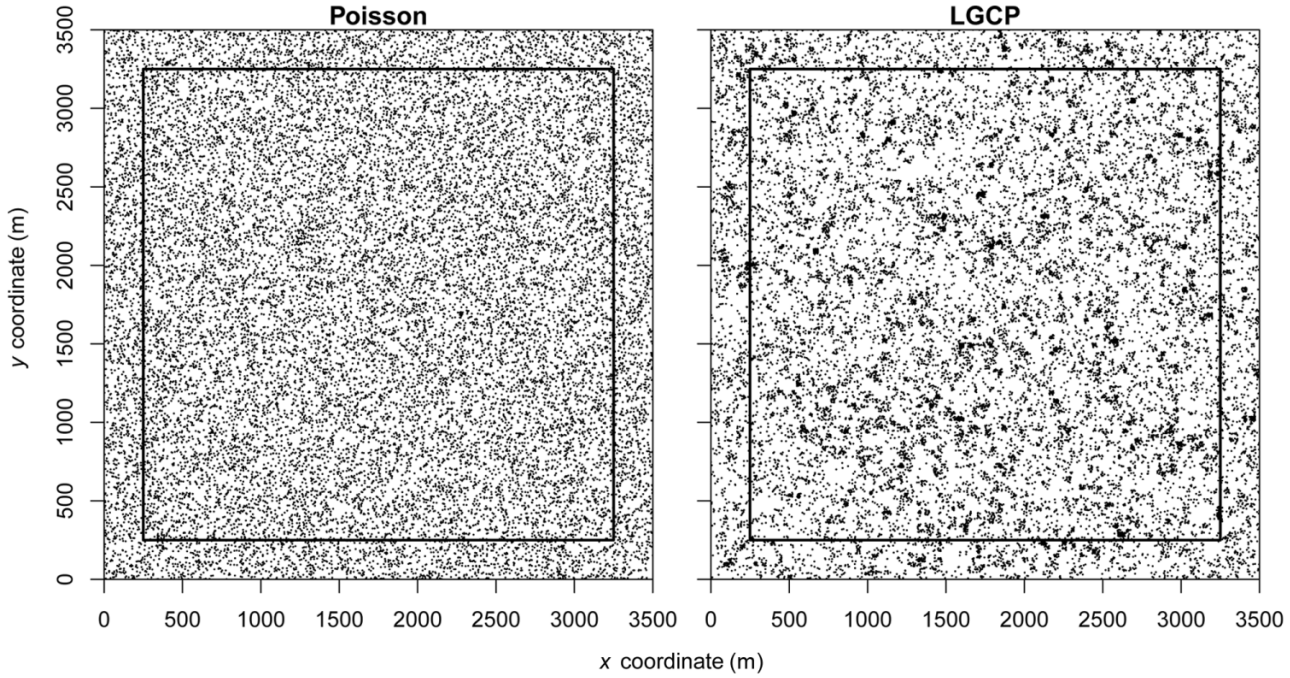

Fig. 5. Pair correlation functions (PCF) of the empirical point pattern and the fitted model.

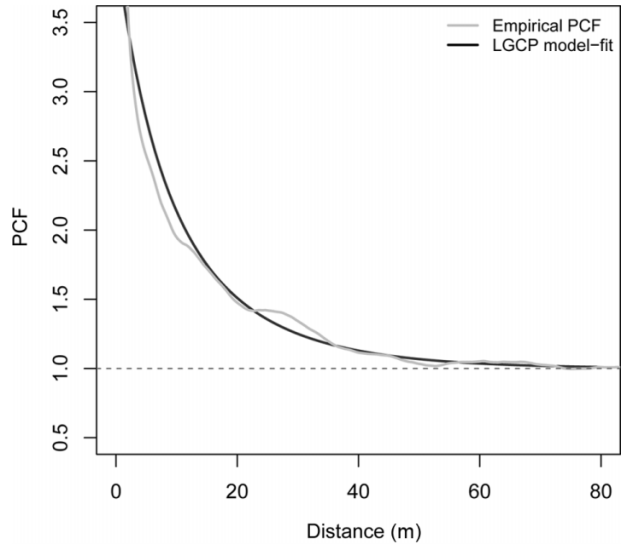

$$\hat{G}(x) = k \sum_{j=1}^{z} \frac{1}{P_{a_j}} \quad [17]$$

if Y is the tree basal area. This reveals why $\hat{G}_{\mathrm{BcACS2}}$ can be expected to be approximately unbiased; it is not strictly unbiased because $g(r)$ in P_{a_j} has to be estimated for eq. [12] and because even an unbiased estimator $\hat{P}_{a_j}$ of P_{a_j} would lead to a biased estimator $1/\hat{P}_{a_j}$ of $1/P_{a_j}$.

However, why should $\hat{G}_{\mathrm{BcACS1}}$ with the expansion factor P_{a_j} replaced by $g(r_{ij})$ also be, at least approximately, unbiased? If $x \in K_j$ for a tree with DBH d_j, its distance r_j to the plot center x is in the interval $0 \le r_j \le R_j$. Under the assumption that tree positions are fixed and that sample points are randomly distributed, it holds

Table 2. Parameters of the simulated point processes.

Parameter	Poisson	LGCP
θ^2	—	1.40
α	—	16.35
μ	—	−7.02
λ	18.01 e−4	18.01 e−4

Note: LGCP, log-Gaussian Cox process.

$$E[g(r_j)|P_{a_j}] = E[g(r_j)|d_j] = \frac{1}{\pi R_j^2} \int_0^{R_j} g(r) 2\pi r \mathrm{d}r = P_{a_j} \quad [18]$$

This is true because in that case the probability of trees of DBH d_j standing in an annulus of radius r and width dr centered at x is $2\pi r\mathrm{d}r/(\pi R_j^2)$. Thus, $\hat{G}_{\mathrm{BcACS1}}$ can also approximately correct for the nondetection bias in ACS because the conditional expectation of $g(r_j)$ given d_j equals P_{a_j}. However, the random variation of $g(r_j)$ around P_{a_j} introduces an additional source of variation into $\hat{G}_{\mathrm{BcACS1}}$ (compared with $\hat{G}_{\mathrm{BcACS2}}$), which must lead to a lower precision of that point estimator. On the other hand, this correction has the advantage that measurement of DBH is not required.

Variance estimation

Under the assumption that the basal area density at each sample plot is measured without error, the variance of $\hat{G}$ can be estimated using the well-known formula

$$\widehat{\mathrm{var}}(\hat{G}) = \frac{1}{n(n-1)} \sum_{i=1}^{n} (G_i - \hat{G})^2 \quad [19]$$

for the variance of the sample mean. Here, G_i represents the terms kz_i, $k \sum_{j=1}^{z_i} [1/\hat{g}(r_{ij})]$, and $k \sum_{j=1}^{z_i} (1/\hat{P}_{a_{ij}})$ from eqs. [3], [10], and [12], respectively. The standard error of $\hat{G}$ can be estimated by

Fig. 6. Point estimators for simple random sampling and Poisson-distributed trees ($k = 1$ for all angle count sampling (ACS) estimators). Density represents the Gaussian kernel density estimation of the probability density function of $\hat{G}$.

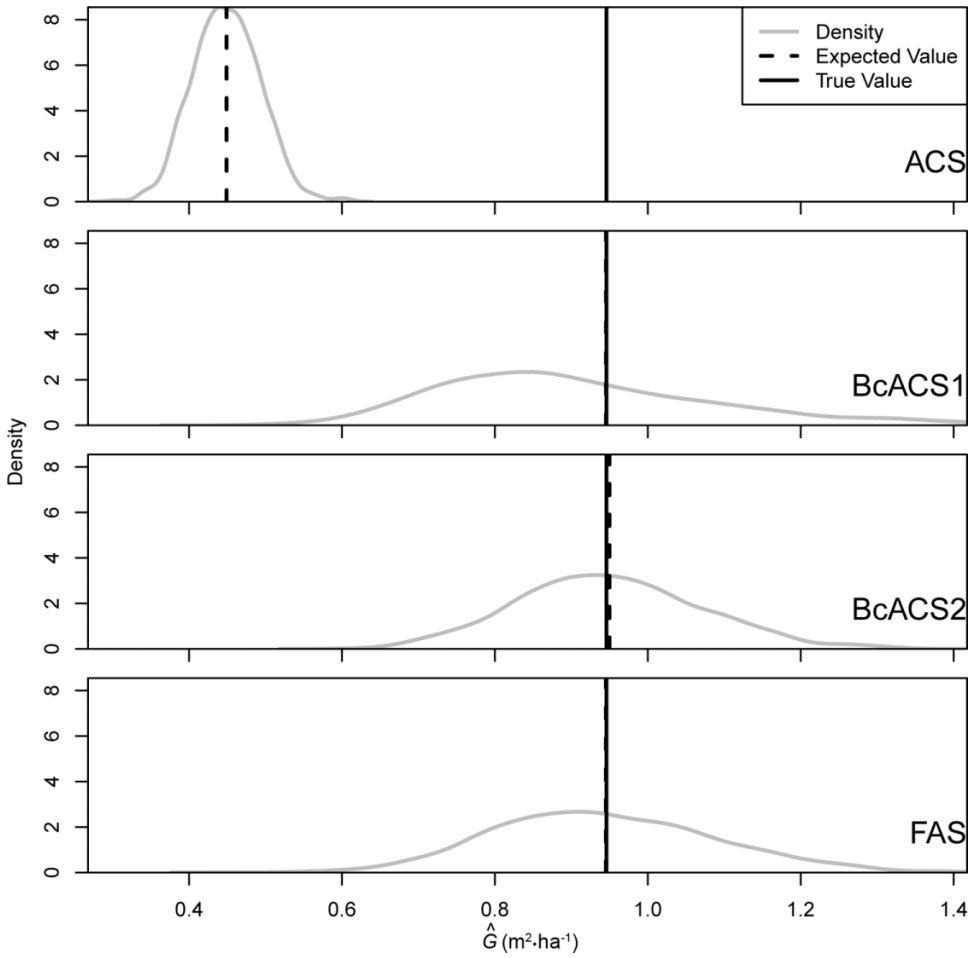

[20] $$\widehat{SE}(\hat{G}) = \sqrt{\widehat{\text{var}}(\hat{G})}$$

As the assumption of error-free measurements will not hold in reality, eqs. [19] and [20] will underestimate variance and standard error (SE), respectively.

Case study A (based on fieldwork)

Data set

Standing deadwood was sampled on 235 plots. We considered every snag or stump having a DBH of at least 7 cm as standing deadwood. We performed PTS as described in the PTS section and used a laser rangefinder to measure the distance from the sample plot to every sighted piece of standing deadwood. Additionally, the DBH of every sighted piece of standing deadwood was obtained by cross calipering, so that the ACS estimator as well as the two BcACS estimators can be applied for different basal area factors ($k = 1$, $k = 2$, and $k = 4$), simply by comparing the radius of the marginal circle $R_{ij} = d_{ij}/(2\sqrt{k})$ and the actual distance r_{ij} of the object to the center of the plot. A piece of standing deadwood was counted if $r_{ij} \leq R_{ij}$. After these measurements, we performed FAS within circular sample plots of a 13 m radius.

The survey area (2416 ha in total) is located in central Germany and covers the forest subdistricts Reinhausen and Sattenhausen of the Lower Saxony State Forest district Reinhausen (51°30′N, 10°00′E).

Sample plots were randomly selected from the phase two plots of the Lower Saxony State Forest inventory, which is carried out as two-phase sampling for stratification (Böckmann et al. 1998; Saborowski et al. 2010). However, in this study we simply treat the sample plots as a completely random sample from a virtual population, because our goal is to compare the different sampling methods rather than producing volume estimates for the study area.

For data analysis we used the software package R (Version 2.14.0; R Development Core Team 2011) and for the analysis of PTS data we used the software Distance (Version 6.0 R2; Thomas et al. 2010).

The best model ($\hat{g}(r) \propto \text{key}(r)[\text{series}(r)]$) for estimating $g(r)$ was selected from all possible combinations of three key functions and two optional series expansions of up to fifth order, based on the minimum AIC (Buckland et al. 2001).

Key functions:

1. Uniform: $\hat{g}(r) = 1/\omega$
2. Half normal: $\hat{g}(r) = e^{\frac{-r^2}{2\sigma^2}}$
3. Hazard rate: $\hat{g}(r) = 1 - e^{-\left(\frac{r}{\sigma}\right)^{-b}}$

Series expansions:

1. Cosine: $\sum_{k=2}^{q} a_k \cos\left(\frac{k\pi r}{\omega}\right)$
2. Simple polynominal: $\sum_{k=2}^{q} a_k \left(\frac{r}{\omega}\right)^{2k}$
3. No series expansion

Results

As standing deadwood is known to be a rare event, it consequently was only observed at some sample plots. The distribution of the observations per plot z_i can be therefore regarded as zero-inflated (Fig. 1). Using PTS, deadwood was observed at 64.7% of all plots, which is the highest fraction of all methods. In contrast, using ACS with $k = 4$, deadwood was only observed at 10.6% of all plots, which is the lowest fraction. The highest maximum number of observations per plot (22) was obtained by PTS, whereas a maximum of only 4 objects per plot was observed using ACS with $k = 4$.

The empirical diameter distributions of standing deadwood sampled with the different techniques is given in Fig. 2. As the diameter has a strong influence on the inclusion probability of objects when using ACS, only the empirical distributions obtained by PTS and FAS can be used to estimate the diameter distribution in the sampling area. These distributions show the classical reverse J-shaped form (Meyer 1952; Nyland 1998).

A half-normal detection function ($\hat{g}(r) = e^{\frac{-r^2}{2\sigma^2}}$) without series expansion was chosen from the AIC-based model selection (Fig. 3). The parameter estimate of the model is $\hat{\sigma} = 12.95$ with $\widehat{SE}(\hat{\sigma}) = 0.43$. The estimated object density (i.e., the number of trees per area unit) is $\hat{D} = 18.63$ ha^{-1} with an estimated standard error $\widehat{SE}(\hat{D}) = 2.08$ ha^{-1}.

The estimated basal area of standing deadwood per area unit ($\hat{G}$) and the corresponding estimated standard errors ($\widehat{SE}(\hat{G})$) are given in Table 1. The smallest $\widehat{SE}(\hat{G})$ (0.059 m^2·ha^{-1}) was obtained by the ACS estimator with $k = 1$, whereas it was largest (0.164 m^2·ha^{-1}) for BcACS2 using $k = 4$. However, at the same time it is obvious that the estimates of G noticeably differ from each other; especially, the estimation obtained by the ACS estimator with $k = 1$ is much smaller than all other estimates.

Discussion

As FAS is known to be theoretically unbiased, we used its estimates of G as a reference for the other methods. However, it must be clearly pointed out that the true value of G is unknown.

Apparently, despite the overlapping approximated 95% confidence intervals constructed by $\hat{G} \pm 1.96\widehat{SE}(\hat{G})$, the estimates of G obtained by ACS using $k = 1$ and $k = 2$ are noticeably smaller than the reference obtained by FAS. We interpret this as a strong hint that ACS suffers from a nondetection bias in this study.

With decreasing k, the difference between the ACS estimates and the FAS reference increases. This is exactly what we expected to occur because, with smaller k, trees at larger distances have to be counted and, from PTS theory, we expected the detection probability to be smaller at larger distances. Thus, with smaller k the proportion of trees that are supposed to be counted by ACS, but are overlooked, increases.

The BcACS estimators generally produce estimates of G showing smaller differences from the FAS reference. Therefore, we anticipate our proposed bias correction to be functional.

Again, the problem of this study based on fieldwork is that the true value of G is unknown and, therefore, we cannot literally assess the nondetection bias, even though there are strong hints that it exists. The same is true for $SE(\hat{G})$, for which the true value is likewise unknown, and, therefore, we cannot make a clear statement about the quality of its estimates.

To overcome these problems, we performed a simulation study as described in the following section.

Case study B (Simulation study)

Point processes

For the simulation study, we simulated positions of standing deadwood as point patterns based upon two different types of underlying point processes.

Table 3. Comparison of the mean estimated basal area of standing dead trees per area unit [$E(\hat{G})$, m^2·ha^{-1}], standard error of the basal area of standing deadwood per area unit [$SE(\hat{G})$, m^2·ha^{-1}], Bias($\hat{G}$) (m^2·ha^{-1}), and root mean square error [RMSE($\hat{G}$), m^2·ha^{-1}] for the different point processes, sampling schemes, and estimators.

Point process	Sampling scheme	Estimator	k	$E(\hat{G})$	$SE(\hat{G})$	Bias($\hat{G}$)	RMSE($\hat{G}$)
Poisson	Random	ACS	1	0.449	**0.044**	−0.497	0.499
		BcACS1	1	0.945	0.293	**−0.001**	0.293
		BcACS2	1	0.950	0.121	0.004	**0.121**
		ACS	2	0.590	0.071	−0.356	0.363
		BcACS1	2	0.948	0.158	0.002	0.158
		BcACS2	2	0.951	0.130	0.005	0.130
		ACS	4	0.717	0.113	−0.229	0.255
		BcACS1	4	0.948	0.167	0.002	0.167
		BcACS2	4	0.949	0.158	0.003	0.158
		FAS	—	0.945	0.148	**−0.001**	0.148
	Systematic	ACS	1	0.449	**0.045**	−0.497	0.499
		BcACS1	1	0.932	0.267	−0.014	0.267
		BcACS2	1	0.945	0.121	−0.001	**0.121**
		ACS	2	0.590	0.072	−0.356	0.363
		BcACS1	2	0.944	0.159	−0.002	0.159
		BcACS2	2	0.947	0.131	0.001	0.131
		ACS	4	0.720	0.110	−0.226	0.252
		BcACS1	4	0.949	0.159	0.003	0.159
		BcACS2	4	0.949	0.151	0.003	0.151
		FAS	—	0.946	0.141	**0.000**	0.141
LGCP	Random	ACS	1	0.449	**0.059**	−0.497	0.501
		BcACS1	1	0.952	0.318	0.006	0.318
		BcACS2	1	0.950	0.149	0.004	**0.149**
		ACS	2	0.589	0.088	−0.357	0.367
		BcACS1	2	0.945	0.184	**−0.001**	0.184
		BcACS2	2	0.951	0.158	0.005	0.158
		ACS	4	0.719	0.127	−0.227	0.260
		BcACS1	4	0.949	0.183	−0.003	0.183
		BcACS2	4	0.952	0.176	0.006	0.176
		FAS	—	0.952	0.167	0.006	0.167
	Systematic	ACS	1	0.449	**0.045**	−0.497	0.499
		BcACS1	1	0.932	0.267	−0.014	0.267
		BcACS2	1	0.945	0.121	−0.001	**0.121**
		ACS	2	0.590	0.072	−0.356	0.363
		BcACS1	2	0.944	0.159	−0.002	0.159
		BcACS2	2	0.947	0.131	0.001	0.131
		ACS	4	0.720	0.110	−0.226	0.252
		BcACS1	4	0.949	0.159	0.003	0.159
		BcACS2	4	0.949	0.151	0.003	0.151
		FAS	—	0.946	0.141	**0.000**	0.141

Note: For any combination of point process and sampling scheme, the values of the best performing estimator in the respective column are highlighted in bold type. k, basal area factor; ACS, angle count sampling; FAS, fixed area sampling; BcACS, bias-corrected angle count sampling estimator; LGCP, log-Gaussian Cox process.

1. A homogeneous Poisson process, to model the case of complete spatial randomness (CSR), widely used as a simple model of spatial distribution. The intensity of the simulated process (Table 2) was derived from the density of standing deadwood in the Hainich data set, a fully mapped 28.2 ha stand in the German National Park Hainich, which was also used in Bäuerle and Nothdurft (2011) to analyze habitat tree locations.
2. A log-Gaussian Cox process (LGCP) to model a heterogeneous population (Fig. 4). Bäuerle and Nothdurft (2011) showed the adequacy of the LGCP model for the reconstruction of habitat tree patterns. Parameters of the simulated process were derived from the Hainich data set by fitting a LGCP model to the empirical point pattern using a minimum contrast approach provided by the R-package spatstat (Baddeley and Turner 2005). The pair correlation functions of the empirical point

Fig. 7. Variance estimates for the different point estimators under the condition of simple random sampling and Poisson-distributed trees ($k = 1$ for all angle count sampling (ACS) estimators). Density represents the Gaussian kernel density estimation of the probability density function of $\widehat{\text{var}}(\hat{G})$. Please note that, for BcACS1, the density is right-truncated at 0.2 for better perceptibility, although it actually ends at 10.76.

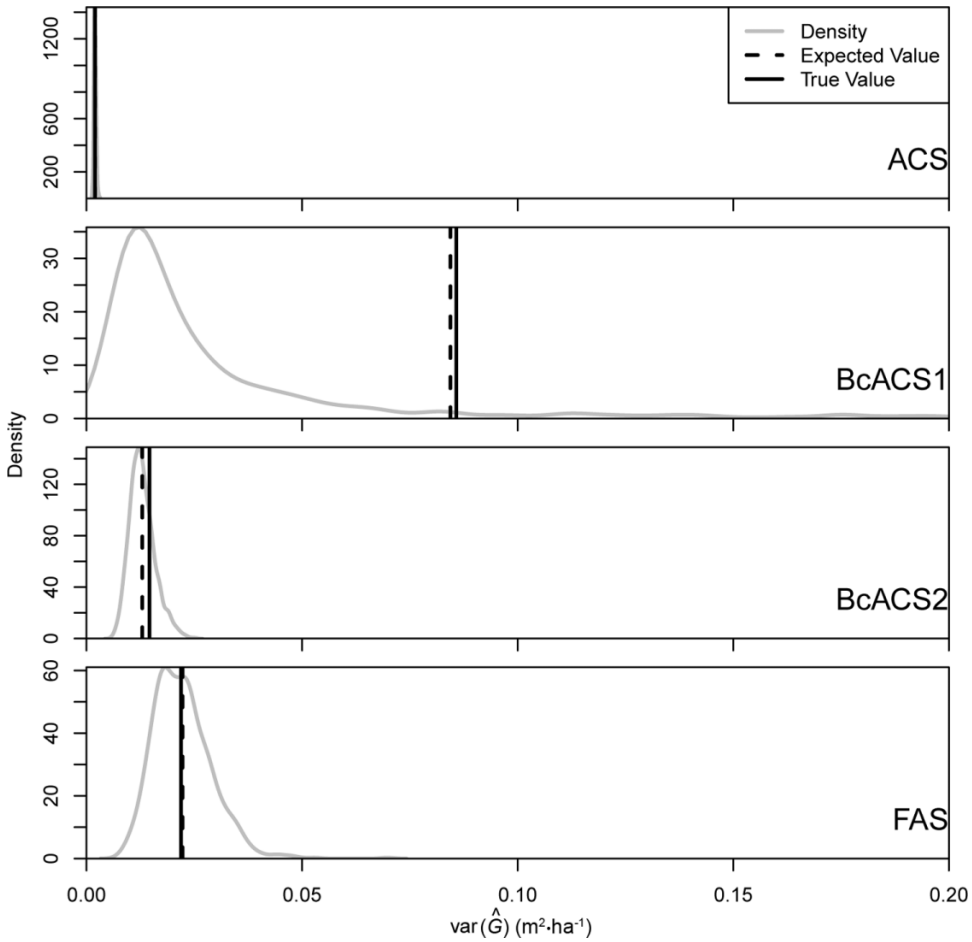

pattern and the fitted model are shown in Fig. 5 and the parameter estimates in Table 2.

Formal definitions of the homogeneous Poisson process and of the LGCP are given in the Appendix.

The spatial distribution of standing deadwood was chosen as an example of a situation where ACS with low basal area factor (e.g., $k = 1$) could be appropriate and nondetection bias is expected to be large as suspected in case study A. We did not model a regular population, because it is very unlikely that rare objects like standing deadwood occur in such patterns.

Diameter distribution

Both point patterns were marked with DBH values from a three-parameter Weibull distribution

$$[21] \qquad f(x;c,b,\theta) = \frac{c}{b}\left(\frac{x-\theta}{b}\right)^{c-1} e^{-\left(\frac{x-\theta}{b}\right)^{c}}$$

which was fitted to the empirical diameter distribution of standing deadwood from the Hainich data set. The estimate of the shape parameter is $c = 0.56$, the estimate of the scale parameter is $b = 9.71$, and the estimate of the location parameter is $\theta = 7.00$.

Simulation program

The simulation study was performed using the software package R (Version 2.14.0; R Development Core Team 2011). Both point processes were simulated in a square window of 3500 m edge length (outer window). To avoid edge effects, 225 sample plots were laid out in a square window of 3000 m edge length (inner window) placed in the center of the outer window. The sample plots were laid out (*i*) on completely randomized positions and (*ii*) on a systematic 200 m × 200 m sampling grid with a random starting point.

The following provides a step-by-step outline of the simulation program:

- Loop (999 runs).
  - Simulate a realization of the point process in the outer window.
  - Mark simulated tree positions randomly with diameter values from the Weibull distribution.
  - Lay out sample plots in the inner window (*i*) at completely random locations (*ii*) on a 200 m × 200 m grid with a random starting point.
  - Calculate the Euclidean distance from every sample plot to every tree.
  - Simulate fixed area sampling with 13 m radius and save results.
  - Simulate ACS and save results; the probability that an object is detected is given by $g(r) = e^{\frac{-r^2}{2\sigma^2}}$, with $\sigma = 12.95$ (the detection function and the parameter estimated in case study A). Further geometrical considerations are not regarded.
  - Estimate the detection function by fitting $\hat{g}(r)$ to the empirical distribution of Euclidean distances from every sample plot to every detected tree.

- Estimate BcACS1 and BcACS2 and save results.
- Calculate the mean of the estimates from the 999 runs.

Results

Point estimates

The performances of the different angle count based estimators (k = 1) and the FAS estimator under the conditions of simple random sampling and Poisson distributed trees is exemplarily depicted in Fig. 6. For detailed statistics see Table 3. It can be seen that the conventional ACS estimator is strongly biased (–0.497 m²·ha⁻¹ (≙–52.5%)), whereas the simulated bias of the theoretically unbiased FAS estimator is extremely small –0.001 m²·ha⁻¹ (≙–0.09%)). The simulated biases of the new estimators BcACS1 (–0.001 m²·ha⁻¹ (≙–0.06%)) and BcACS2 (0.004 m²·ha⁻¹ (≙0.42%)) are also negligibly small.

The root mean square error (RMSE) of the conventional ACS estimator is 0.499 m²·ha⁻¹ (≙52.7%) and, therefore, much larger than that of BcACS1 (0.293 m²·ha⁻¹ (≙31.0%)) and that of BcACS2 (0.121 m²·ha⁻¹ (≙12.8%)), even though the new estimators have higher SEs than the conventional one. The RMSE of the FAS estimator is 0.148 m²·ha⁻¹ (≙15.7%).

For the sake of brevity, the performance of the different estimators under varying conditions is not outlined in detail, but given in Table 3. For all simulated cases, the conventional ACS estimator is strongly biased, especially for k = 1. Both new BcACS estimators as well as the FAS estimator are (approximately) unbiased in all simulated cases.

The trend found in case study A is also observed in case study B. With decreasing k the advantage of the corrected estimators increases. For all k, BcACS2 achieved a lower RMSE than the other two angle count methods. For k = 1 and k = 2, BcACS2 is also more precise than FAS. The absolutely smallest RMSE can be achieved using the BcACS2 estimator with k = 1.

Variance estimates

The performance of the variance estimator (eq. [19]) for the different point estimates under the conditions of simple random sampling and Poisson-distributed trees is exemplarily depicted in Fig. 7.

The variance estimates for ACS and FAS are approximately unbiased, whereas there is a small negative bias for BcACS1 (–0.0014 m⁴·ha⁻²) and BcACS2 (0.0017 m⁴·ha⁻²).

The RMSE of the variance estimation is smallest for ACS (0.0004 m⁴·ha⁻²), whereas it is by far largest for BcACS1 (0.2208 m⁴·ha⁻² (≙257.53%)) due to the extremely high SE of this estimator. The RMSE of the variance estimation is 0.0017 m⁴·ha⁻² for BcACS2 and 0.0004 m⁴·ha⁻² for FAS.

For the sake of brevity, the performance of the variance estimator for the different point estimators under varying conditions is given in Table 4. It can be seen that, under all conditions, the RMSE of the variance estimator is smallest for the conventional ACS estimator. However, it increases with increasing k. In almost all cases the RMSE of the variance estimator is smaller for BcACS2 than for BcACS1. Especially with small k, the difference becomes very pronounced.

Table 4. Comparison of the mean estimated variance of the basal area of standing dead trees per area unit [$E[\widehat{\mathrm{var}}(\hat{G})]$, m²·ha⁻¹], standard error of the estimated variance [$\mathrm{SE}[\widehat{\mathrm{var}}(\hat{G})]$, m²·ha⁻¹], $\mathrm{Bias}[\widehat{\mathrm{var}}(\hat{G})]$ (m²·ha⁻¹), and root mean square error of the estimated variance [$\mathrm{RMSE}[\widehat{\mathrm{var}}(\hat{G})]$, m²·ha⁻¹] for the different point processes, sampling schemes, and estimators.

Point process	Sampling scheme	Estimator	k	E [$\widehat{\mathrm{var}}(\hat{G})$]	SE [$\widehat{\mathrm{var}}(\hat{G})$]	Bias [$\widehat{\mathrm{var}}(\hat{G})$]	RMSE [$\widehat{\mathrm{var}}(\hat{G})$]
Poisson	Random	ACS	1	0.0020	0.0000	0.0000	0.0000
		BcACS1	1	0.0844	0.2208	–0.0014	0.2208
		BcACS2	1	0.0129	0.0000	–0.0017	0.0017
		ACS	2	0.0052	0.0000	0.0004	0.0004
		BcACS1	2	0.0237	0.0004	–0.0011	0.0011
		BcACS2	2	0.0161	0.0000	–0.0009	0.0009
		ACS	4	0.0127	0.0000	–0.0004	0.0004
		BcACS1	4	0.0256	0.0004	–0.0024	0.0024
		BcACS2	4	0.0236	0.0000	–0.0015	0.0015
		FAS	—	0.0223	0.0000	0.0003	0.0003
	Systematic	ACS	1	0.0020	0.0000	0.0000	0.0000
		BcACS1	1	0.0711	0.1044	–0.0002	0.1044
		BcACS2	1	0.0128	0.0000	–0.0018	0.0018
		ACS	2	0.0052	0.0000	0.0000	0.0000
		BcACS1	2	0.0238	0.0004	–0.0015	0.0015
		BcACS2	2	0.0159	0.0000	–0.0012	0.0012
		ACS	4	0.0128	0.0000	0.0006	0.0006
		BcACS1	4	0.0255	0.0000	0.0001	0.0001
		BcACS2	4	0.0235	0.0000	0.0007	0.0007
		FAS	—	0.0222	0.0000	0.0025	0.0025
LGCP	Random	ACS	1	0.0034	0.0000	–0.0004	0.0004
		BcACS1	1	0.0924	0.1576	–0.0085	0.1578
		BcACS2	1	0.0183	0.0004	–0.0038	0.0038
		ACS	2	0.0078	0.0000	0.0000	0.0000
		BcACS1	2	0.0286	0.0003	–0.0051	0.0051
		BcACS2	2	0.0221	0.0004	–0.0028	0.0028
		ACS	4	0.0171	0.0001	0.0009	0.0009
		BcACS1	4	0.0324	0.0002	–0.0009	0.0010
		BcACS2	4	0.0309	0.0002	–0.0000	0.0002
		FAS	—	0.0294	0.0001	0.0014	0.0014
	Systematic	ACS	1	0.0034	0.0000	–0.0001	0.0001
		BcACS1	1	0.1304	0.7916	–0.0052	0.7917
		BcACS2	1	0.0181	0.0004	–0.0044	0.0044
		ACS	2	0.0078	0.0000	–0.0004	0.0004
		BcACS1	2	0.0301	0.0005	–0.0040	0.0041
		BcACS2	2	0.0219	0.0001	–0.0035	0.0035
		ACS	4	0.0170	0.0000	–0.0012	0.0012
		BcACS1	4	0.0321	0.0002	–0.0042	0.0043
		BcACS2	4	0.0305	0.0001	–0.0038	0.0038
		FAS	—	0.0292	0.0002	0.0017	0.0017

Note: k, basal area factor; ACS, angle count sampling; FAS, fixed area sampling; BcACS, bias-corrected angle count sampling estimator; LGCP, log-Gaussian Cox process.

Discussion

We simulated two different point processes, the Poisson process as a null model for the case of CSR, and the LGCP as a model for a clustered population. The simulated point processes were randomly marked with diameter values from a Weibull distribution, i.e., the marks are independent. According to Illian et al. (2008), the independent marking model may be regarded as a null model for marked point processes. Undoubtedly, other possible populations exist that differ in their point process, their diameter distribution, and their dependency of the marks. However, because of the sound theoretical reasoning for the corrected estimators, we are confident that the observed trends are also valid for other populations.

To simulate the detection probability, we used the detection function derived from case study A. The function is quite steep around r = 10 m (Fig. 3). This is not surprising, because in the beech (*Fagus sylvatica* L.) dominated sampling area, sight is often limited by a dense understory. However, in forests with less dense understory the sight is less limited, so that the detection probability is certainly higher there. A higher detection probability obviously comes along with a lower nondetection bias of ACS, so that the advantages of the new estimators may be less prominent under these conditions.

The variance estimations for BcACS1 and BcACS2 show a small negative bias. This may be due to the assumption of error-free measurement of G_i, when eq. [19] is applied for variance estimation. However, this assumption is violated for BcACS1 and BcACS2, as the variation introduced by modeling $g(r)$ and P_a,

respectively, is not considered. Thus, further research is required to develop unbiased variance estimators for BcACS1 and BcACS2.

Conclusion

Both new estimators (BcACS1 and BcACS2) proved to be practicable during the field work and provide approximately unbiased point estimates. In contrast, the ACS estimator is strongly biased in our study. The size of the bias depends on the detection probability and on the counting angle. Especially if a small counting angle is used and in cases of limited sight conditions (e.g., owing to a dense understory), the new estimators should therefore be preferred to the conventional ACS estimator.

The RMSE of BcACS2 is smaller than that of BcACS1, which was expected because $g(r)$ is only an estimate for the correct bias correction by $P_{a_{ij}}$. Moreover, the variance estimation works much better for BcACS2 than for BcACS1. However, additional sampling effort for BcACS2 is much higher than for BcACS1, unless diameters are measured for other reasons anyway. If this is the case, BcACS2 should be preferred to BcACS1, otherwise time studies are needed to evaluate if the smaller RMSE and better variance estimation of BcACS2 compensates for the extra sampling effort.

A limitation of the new estimators is given by the necessary sample size. As the detection function $g(r)$ has to be fitted to the empirical data, a certain number of sighted objects m is needed. As a rule of thumb, m generally should be at least 60–80 (Buckland et al. 2001). The number of necessary sample plots therefore depends on the number of sighted objects per plot.

Acknowledgments

We gratefully acknowledge the support of the German Research Foundation (Deutsche Forschungsgemeinschaft, DFG) under grant number SA415/4-1. We thank Jürgen Bauhus (University of Freiburg) and Christian Wirth (University of Leipzig) for providing the Hainich data set. We are grateful to the Lower Saxony State Forests (Niedersächsische Landesforsten) for the opportunity to work on their sites and for providing forest management planning data. We would like to thank retired district forest officer Otto Beck and forest rangers Harald Höhne and Henning Freiesleben for their hospitality and cooperation. We thank André Hardtke, Garlef Kalberlah, Birte Krause, and Phillip Schlotzhauer for their assistance during the fieldwork, and Frauke Thorade for proofreading the manuscript. We thank two anonymous reviewers and the Associate Editor for their useful comments and suggestions.

References

Baddeley, A., and Turner, R. 2005. spatstat: an R package for analyzing spatial point patterns. J. Stat. Softw. **12**: 1–42.

Bäuerle, H., and Nothdurft, A. 2011. Spatial modeling of habitat trees based on line transect sampling and point pattern reconstruction. Can. J. For. Res. **41**(4): 715–727. doi:10.1139/x11-004.

Bitterlich, W. 1952. Die Winkelzählprobe Ein optisches Messverfahren zur raschen Aufnahme besonders gearteter Probeflächen fiir die Bestimmung der Kreisflächen pro Hektar an stehenden Waldbeständen. Forstwiss. Centralbl. **71**(7–8): 215–225. doi:10.1007/BF01821439.

Bitterlich, W. 1984. The relascope idea: relative measurements in forestry. Commonwealth Agricultural Bureaux, Slough, UK.

Böckmann, T., Saborowski, J., Dahm, S., Nagel, J., and Spellmann, H. 1998. Die Weiterentwicklung der Betriebsinventur in Niedersachsen. Forst und Holz, **53**(8): 219–226.

Buckland, S., Anderson, D., Burnham, K., Laake, J., Borchers, D., and Thomas, L. 2001. Introduction to distance sampling: estimating abundance of biological populations. Oxford University Press, Oxford.

Buckland, S., Anderson, D., Burnham, K., Laake, J., Borchers, D., and Thomas, L. 2004. Advanced distance sampling: estimating abundance of biological populations. Oxford University Press, Oxford.

Fewster, R.M., Buckland, S.T., Burnham, K.P., Borchers, D.L., Jupp, P.E., Laake, J.L., and Thomas, L. 2009. Estimating the encounter rate variance in distance sampling. Biometrics, **65**(1): 225–236. doi:10.1111/j.1541-0420.2008.01018.x.

Gabler, K., and Schadauer, K. 2006. Methoden der Österreichischen Waldinventur 2000/02. Grundlagen, Entwicklung, Design, Daten, Modelle, Auswertung und Fehlerrechnung. Institut für Waldinventur Bundesforschungs- und Ausbildungszentrum für Wald, Naturgefahren und Landschaft, Wien, BFW-Berichte 135.

Gove, J., Ducey, M., Ståhl, G., and Ringvall, A. 2001. Point relascope sampling — A new way to assess downed coarse woody debris. J. For. **99**: 4–11.

Gregoire, T.G., and Valentine, H.T. 2008. Sampling strategies for natural resources and environment. Chapmann and Hall/CRC, Boca Raton, Fla.

Illian, J., Penttinen, A., and Stoyan, D. 2008. Statistical analysis and modelling of spatial point patterns. John Wiley and Sons, New York.

Kändler, G., 2009. The design of the second German National Forest Inventory. *In* Proceedings of the Eighth Annual Forest Inventory and Analysis Symposium, Monterey, Calif., 16–19 October 2006. *Edited by* R.E. McRoberts, G.A. Reams, P.C. Van Deusen, and W.H. McWilliams. USDA For. Serv., Washington, D.C., Gen. Tech. Rep. No. WO-79. pp. 19–24.

Mandallaz, D. 2008. Sampling techniques for forest inventories. Chapman and Hall/CRC, Boca Raton, Fla.

MCPFE. 2002. Background information for improved Pan-European indicators for sustainable forest management. Report, Ministerial Conference on the Protection of Forests in Europe (MCPFE) Liaison Unit, Vienna.

MCPFE. 2003. State of Europe's forests 2003: the MCPFE report on sustainable forest management in Europe. Report, Ministerial Conference on the Protection of Forests in Europe (MCPFE) Liaison Unit, Vienna; United Nations Economic Commission for Europe/Food and Agricultural Organization (UNECE/FAO).

Meyer, H.A. 1952. Structure, growth, and drain in balanced, uneven-aged forests. J. For. **52**: 85–92.

Meyer, P. 1999. Totholzuntersuchungen in nordwestdeutschen Naturwäldern: Methodik und erste Ergebnisse. Forstwiss. Centralbl. **118**: 167–180. doi:10.1007/BF02768985.

Møller, J., and Waagepetersen, R. 2003. Statistical inference and simulation for spatial point processes. Chapman and Hall, Boca Raton, Fla.

Nyland, R.D. 1998. Selection system in northern hardwoods. J. For. **96**: 18–21.

Polley, H. (*Editor*). 2005. Die zweite Bundeswaldinventur - BWI² - Der Inventurbericht. Bundesministerium für Ernährung, Landwirtschaft und Verbraucherschutz.

R Development Core Team. 2011. R: a language and environment for statistical computing. R Foundation for Statistical Computing, Vienna, Austria. ISBN 3-900051-07-0.

Ritter, T., and Saborowski, J. 2012. Point transect sampling of deadwood: a comparison with well-established sampling techniques for the estimation of volume and carbon storage in managed forests. Eur. J. For. Res. **131**(6): 1845–1856. doi:10.1007/s10342-012-0637-2.

Rondeux, J., and Sanchez, C. 2010. Review of indicators and field methods for monitoring biodiversity within national forest inventories. Core variable: Deadwood. Environ. Monit. Assess. **164**(1–4): 617–630. doi:10.1007/s10661-009-0917-6.

Saborowski, J., Marx, A., Nagel, J., and Boeckmann, T. 2010. Double sampling for stratification in periodic inventories — Infinite population approach. For. Ecol. Manag. **260**(10): 1886–1895. doi:10.1016/j.foreco.2010.08.035.

Schadauer, K., Gschwantner, T., and Gabler, K. 2007. Austrian National Forest Inventory: caught in the past and heading toward the Future. *In* Proceedings of the Seventh Annual Forest Inventory and Analysis Symposium, Portland, Maine, 3–6 October 2005. *Edited by* R. McRoberts, G. Reams, P. Van Deusen, and W. McWilliams. USDA For. Serv., Washington, D.C., Gen. Tech. Rep. No. WO-77. pp. 47–53.

Seber, G., 1982. The estimation of animal abundance and related parameters. Macmillian, New York.

Thomas, L., Buckland, S., Rexstad, E., Laake, J., Strindberg, S., Hedley, S., Bishop, J., Marques, T., and Burnham, K. 2010. Distance software: design and analysis of distance sampling surveys for estimating population size. J. Appl. Ecol. **47**: 5–14. doi:10.1111/j.1365-2664.2009.01737.x.

Tomppo, E. 2009. The Finnish National Forest Inventory. In Proceedings of the Eighth Annual Forest Inventory and Analysis Symposium, Monterey, Calif., 16–19 October 2006. *Edited by* R.E. McRoberts, G.A. Reams, P.C. Van Deusen, and W.H. McWilliams. USDA For. Serv., Washington, D.C., Gen. Tech. Rep. No. WO-79. pp. 39–46.

Woodall, C., Rondeux, J., Verkerk, P., and Ståhl, G. 2009*a*. Estimating dead wood during national forest inventories: a review of inventory methodologies and suggestions for harmonization. Environ. Manage. **44**(4): 624–631. doi:10.1007/s00267-009-9358-9.

Woodall, C., Verkerk, H., Rondeux, J., and Ståhl, G. 2009*b*. Who's counting deadwood. EFI News, **17**(2): 12–13.

Appendix

Definition of a homogeneous Poisson process

A homogeneous Poisson process N is characterized by two fundamental properties (Illian et al. 2008).

1. The number of points of N in any bounded set B follows a Poisson distribution with mean $\lambda\nu(B)$, where λ is the intensity of the point process and $\nu(B)$ is the area of B.

2. The number of points of N in k disjoint sets form k independent random variables.

Definition of a log-Gaussian Cox process (LGCP)

Cox processes are a class of spatial point process models describing clustering resulting from environmental variability (Illian et al. 2008). They are a generalization of inhomogeneous Poisson processes, where the intensity function $\lambda(x)$ is random. A Cox process can be regarded as the result of a two-stage random mechanism and is therefore sometimes called the doubly stochastic Poisson process (Illian et al. 2008). A Cox point process model is defined in two steps: First consider a stationary non-negative valued random field $\{\Lambda(x)\}$. Second, given a realization $\{\lambda(x)\}$ of $\{\Lambda(x)\}$, the points of the corresponding realization of the Cox process form an inhomogenous Poisson process with intensity function $\lambda(x)$ (Illian et al. 2008).

If $\{Z(x)\}$ is a stationary and isotropic Gaussian random field, its distribution is specified by the mean $\mu = EZ(x)$, the variance $\theta^2 = \mathrm{var}[Z(x)]$, and the spatial correlation function $\rho(x_1, x_2) = \mathrm{Cov}[Z(x_1), Z(x_2)]/\theta^2$. An LGCP is an inhomogeneous Poisson process with a random intensity process

[A1] $$\Lambda(x) = \exp[Z(x)]$$

(Illian et al. 2008). The intensity of the process according to Møller and Waagepetersen (2003) is then

[A2] $$\lambda = E\Lambda(x) = \exp\left(\mu + \frac{\theta^2}{2}\right)$$